

Enhanced antitumor effect of curcumin loaded solid lipid nanoparticles in Dalton's ascites lymphoma mice

Krishnaveni P¹, Thangapandiyam M^{3*}, Raja P² & Rao GVS¹

¹Department of Veterinary Pathology; ²Department of Animal Biotechnology, Madras Veterinary College, Tamil Nadu Veterinary and Animals Sciences University, Chennai - 600 007, Tamil Nadu, India

³Veterinary Clinical Complex, Veterinary College and Research Institute, Tamil Nadu Veterinary and Animals Sciences University, Udumalpet - 642 126, Tamil Nadu, India

Received 03 August 2022; revised 16 November 2022

Curcumin is widely known for its antibacterial, antioxidant and anti-inflammatory effects and has been reported to possess anticancerous activity as well. However, its medical application is limited because of poor bioavailability and rapid metabolism. In this study, we encapsulated curcumin in solid lipid nanoparticles and studied its anticancerous effect in Dalton's Ascites Lymphoma (DAL) mice model. The physicochemical characteristics of curcumin solid lipid nanoparticles (CUR-SLN) were assessed and the anticancer efficacy was determined by *in vivo* studies. The curcumin solid lipid nanoparticles were synthesized by solvent emulsification evaporation method with particle size less than 100 nm. Antitumor effect of nanocurcumin (50 mg/kg) and curcumin (100 mg/kg) was evaluated in Dalton's Ascites Lymphoma bearing mice. Pathological and immunohistochemical parameters were studied. Mean survival time and percentage increase in lifespan were assessed. Nanocurcumin group showed more significant influence in reducing tumor volume and weight, inducing apoptosis, reducing angiogenesis and invasion restoring antioxidant parameters and increased mean survival time. Curcumin and nanocurcumin inhibited the activation of nuclear factor-kappa B (Nf-kB), and thereby proved the pathway by which it induced anti-angiogenic and anti-invasive property.

Keywords: Antiangiogenic, Anti-invasive, *Curcuma longa*, Nanocurcumin, Solvent emulsification evaporation method, Turmeric

Cancer, a multifactorial, multistep disease of genome characterized by alteration in gene expression ranks as a leading cause of death now a day. The global cancer burden is expected to be 28.3 million by 2040, about 40% rise from 2020. Lymphoma heterogeneous group of disorder constitute 3% of all malignancies¹. Non-Hodgkin's Lymphoma is responsible for 80,470 new cases and 20,250 deaths in US 2022². In India, the incidence rate is estimated to be 3.5 and 3.6/100000 for men and women, respectively¹. Even though it is considered to be one of the most chemotherapy sensitive neoplasms, prognosis is often variable. Most of the anticancer drugs used currently lack specificity, leading to systemic toxicity and adverse effects³. Dietary phytochemicals have gained importance in recent years in cancer chemotherapy. Dietary polyphenols have been found to possess potential preventive as well as therapeutic effects by interfering with initiation, promotion and progression of cancer.

Curcumin is a natural polyphenolic compound obtained from *Curcuma longa* L. been shown to inhibit initiation, progression and metastasis of cancers^{4,5}. Besides its anticancerous property curcumin possess anti-inflammatory and antioxidant effects⁶. Curcumin exerts its anticancerous effect by acting through various signaling pathways, inhibiting cell proliferation, downregulating various transcription factors Nuclear factor-kappa B (Nf-kB), activator protein-1 (AP-1), and Early growth response factor-1 (Egr-1), invasion, angiogenesis (Vascular endothelial growth factor) metastasis, induction of apoptosis and inflammation (TNF, COX2 and IL-1)^{4,7}. However, curcumin has low aqueous solubility and rapid systemic elimination which limits its bioavailability. Hence, there is an urgent need for developing formulations which can improve its clinical efficacy.

Previous studies have demonstrated that nanoparticle encapsulation can improve the oral bioavailability of curcumin⁸. Nanocarriers are frequently investigated as a potential tumor targeting vehicles because of their ability to accumulate in the

*Correspondence:
E-Mail: sugigold@gmail.com

tumor sites because of leaky microvasculature³. Solid lipid nanocarriers combine advantages and avoid the disadvantages of other colloidal carriers like controlled drug release and drug targeting, increased drug stability, incorporation of lipophilic and hydrophilic drugs, no toxicity of carrier and suitable for large scale production and sterilization⁹. In this context, here, we encapsulated curcumin in solid lipid nanocarriers, and explored the antitumor activity of 'curcumin loaded solid lipid nanoparticles (CUR-SLN)' using Dalton's Ascites Lymphoma (DAL) cells by *in vivo* methods.

Materials and Methods

Synthesis of curcumin solid lipid nanoparticles

Curcumin (Sigma catalogue no: 1386, >65% assay 10 g) obtained from M/s Sigma Aldrich, Glyceryl monostearate, lecithin soya, Tween 80 and chloroform were used for the synthesis of nanoparticles. CUR-SLN was prepared by solvent emulsification evaporation method¹⁰. Briefly, 100 mg glyceryl monostearate and 40 mg lecithin soya mixed in 1 mL chloroform which formed phase A, 12 mg curcumin was dissolved in 2 mL chloroform which constitute phase B. Phase A and B solutions were completely mixed to get a uniform miscible solution and it forms the organic phase. It was transferred to the aqueous phase containing 10 mL of surfactant solution (1.5% Tween 80). The resultant mixture was homogenized for 5 min followed by sonication for 20 min (750 Watts at 75% amplitude). Finally, the solution was stirred with magnetic bead for 3 h at 1000 rpm in dark room. This solution was converted to powder using lyophilizer and kept at room temperature (29°C). Blank SLN (B-SLN) was prepared without adding curcumin.

Characterization of nanoparticles

Particle size, Polydispersity index (PDI) and Zeta potential

Particle size polydispersity index and zeta potential were measured using Zetasizer (ZEN3600, Malvern Instrument, UK) based on the nature of nanosuspension. The SLN suspensions were diluted in triple distilled water in 1:10 proportion for characterization of nanoparticles. About 500 μ L of CUR-SLN suspension was diluted in 4500 μ L of triple distilled water and ultrasonicated for 3 h before measuring the particle size.

Scanning Electron Microscopy (SEM)

The surface morphology of the raw curcumin and curcumin solid lipid nanoparticles was analyzed by

SEM (FEI QUANTA FEG 200F, SAIF- IIT, Madras). Raw curcumin and lyophilized samples of CUR-SLN were sputter coated with gold and subjected to SEM analysis. The images were captured at 6000X magnification.

Fourier transform infrared spectroscopy (FTIR)

Curcumin, blank SLNPs and curcumin-SLNPs were crushed with potassium bromide (KBr) to get the pellets by applying a pressure of 300 kg/cm². FTIR spectra of the above sample were obtained by averaging 32 interferograms with resolution of 2 cm⁻¹ in the range of 1000-4000 cm⁻¹.

In vivo study

Maintenance of animals and induction of Dalton's Lymphoma

Male BALB/c mice (6 weeks) of 20-25 g procured from Biogen laboratory animal facility, Bangalore, India for *in vivo* study. Experimental animals were housed in sterile polypropylene cages and maintained under standard laboratory conditions (Temperature 22±2°C, humidity 50±5% and 12 h dark/light cycle) and fed with standard laboratory animal pellet feed and water. They were allowed to acclimatize to the environment for 7 days prior to the experimental period. Randomization was done based on the body weight and animals were grouped in to four groups (Mean body weight variation < 20%). DAL cell lines were procured from Amala Cancer Research Center, Kerala, India. Ascites model was induced by inoculation of 1×10⁶ cells in 0.1 mL intraperitoneally. Solid model was developed by injecting the cells intramuscularly in the right thigh region. Routine clinical examination of all animals was performed throughout the experimental period.

Experimental design

Experimental animals were randomly divided in to two models I- Ascites model and II- solid model each having four groups with 12 animals each. Experimental design used in this study was approved by the Institutional Animal Ethics Committee, Madras Veterinary College, Chennai (Approval number 04/SA/IAEC/2021). Six animals were kept as normal control group common to both ascites and solid model. Treatment with methotrexate, curcumin and curcumin-SLN were started from 24th h of tumor induction and were continued for 15 days. The protocol was as follows. (Table 1)

On 16th day, six animals from each group were sacrificed. The remaining six animals in each group were left as such and continued with respective

Table 1 — Experimental design

Groups	No. of animals		Treatment
	Treatment	Mean survivaltime	
I	6	6	DAL control group. [DAL cells (1×10^6 cells) inoculated intraperitoneally and intramuscularly for ascites and solid model, respectively without treatment]
II	6	6	DAL+Methotrexate. [Methotrexate (3.5mg/kg) in milli-q- water given orally from 24 h after inoculation of DAL, once a day throughout the experimental period in both models]
III	6	6	DAL+Curcumin. [Curcumin at 100 mg/kg b.wt with corn oil given orally from 24 h of inoculation of DAL , once a day throughout the experimental period in both models]
IV	6	6	DAL+Nanocurcumin. [Nanocurcumin at 100 mg/kg b.wt in milli-q-water given orally from 24 h of inoculationof DAL, once a day throughout the experimental period in both models]

treatments and recorded mean survival time. Peritoneal fluid was collected for assessing the tumor volume. Peritoneal membrane and other visceral organs were collected for histopathological and immunohistochemical studies. In solid tumor model, after sacrificing the animals, the tumor volume was recorded and tumor sample was collected in 10%NBF with other visceral organs for histopathology and immunohistochemistry.

Bodyweight

Each mouse was weighed before the induction of tumor and just before the sacrifice to record the initial and final bodyweight. Increase in bodyweight was calculated based on the following formula.

Increase in body wt. (in g) = Final body wt. – Initial body wt .

Tumor volume and weight

In ascitic model, the whole ascitic fluid from each animal was collected using 22-gauge syringe and transferred in to a weighed graduated centrifuge tube and measured the volume and weight of ascitic fluid. In solid tumor model diameter of the excised tumor tissue was determined by vernier caliper and tumor volume was calculated by the following formula¹¹:

$V = 4/3 \pi r_1^2 \times r_2$, where, r1 and r2 are radii of tumors at two different planes.

Weight of the excised mass was also measured.

Cytology of ascitic fluid

Cytology samples were obtained by fine needle aspiration from ascitic abdomen. A drop of ascitic fluid smeared over clean, grease free microscopic slides and thin smears were made. The smears prepared were either air dried and stained with Leishman-Geimsa stain immediately.

Histopathology

Peritoneum, excised solid tumor samples and internal vital organs were used for histopathological studies. They were collected and fixed in 10 %NBF for 48 h and then processed, embedded in paraffin and

4 to 5 μm thick sections were made. Tissue sections were stained using Hematoxylin and Eosin (H&E) and observed under the microscope (Olympus CX43)¹².

Microvessel density (MVD) and diameter evaluation

Neovessel formation in the peritoneal lining was observed and documented. Peritoneal tissue sections were processed for H&E stain and MVD/hpf was quantified manually¹³. Microvessel diameter (μm) was determined using Magvision Magcam software.

Immunostaining

Immunological detection of CD31 (Cluster of differentiation 31), MMP 9 (Matrix metalloproteinase-9) and COX-2 (Cyclooxygenase 2) antibodies were made in the formalin fixed sections of peritoneum. Air dried smears of ascitic fluid were taken in poly L lysine coated slides of the tumor control and treatment groups, and immunostaining for Nf-kB was performed using specific antibodies as per manufactures instructions.

Mean survival time (MST) and percentage increase in lifespan (ILS)

Six animals in each group of both the models were maintained with continuing respective treatment till survival. Mean survival period was recorded and expressed as mean survival time in days. The percent increase in lifespan was calculated as follows¹⁴.

$MST = \Sigma \text{ survival time (days) of each mouse in a group} / \text{Total number of mice}$

$ILS = [\text{Mean survival time of treated group}] / (\text{Mean survival time of tumor control group}) \times 100 - 100$

Statistical analysis

The data generated from different parameters of experimental study were subjected to one way analysis of variance (ANOVA), followed by the Duncan's multiple range test and Kaplan Meier survival analysis was used for MST. Analysis was performed by using IBM SPSS software version 26

for windows. The difference among the groups were considered significant when $P < 0.05$.

Results

Characterization of CUR-SLN

The CUR-SLN showed the in mean particle size of 91.1 ± 7.5 nm, PDI of 0.367 and zeta potential of -37.6 mv (Fig. 1 A-B). The optimized size of blank solid lipid nanoparticles (BSLN) was 106.7 ± 34.9 nm, PDI was 0.319 and zeta potential was -40.8 mv (Fig. 1 C-D). Scanning Electron Microscopy studies of CUR-SLN revealed smooth surface morphology whereas curcumin revealed rough surface (Fig. 2). In Fourier transform infrared spectroscopy analysis spectrum of curcumin, Cur-SLN and Blank-SLN was shown in Fig. 3. FTIR spectra of curcumin revealed the characteristic peak at 3507 cm^{-1} of O-H and 2968 cm^{-1} and 2880 cm^{-1} for C-H stretching vibration. In B-SLN, the characteristic peak was present at 3353 cm^{-1} and 2967 cm^{-1} corresponding to O-H and C-H bond stretching. The CUR-SLN showed common peak with blank solid lipid nanoparticles at 3355 cm^{-1} and with curcumin at 2966 cm^{-1} and 2879 cm^{-1} .

In vivo antitumor effects

Body weight

A significant increase in body weight was observed in DAL induced control animals as compared to

normal control animals. The methotrexate and curcumin treated group showed reduction in bodyweight gain. As compared to other treatment groups, the nanocurcumin group showed significant reduction in body weight gain (Fig. 4).

Tumor volume and weight

The methotrexate group showed decreased tumor volume as compared to the tumor control group. The tumor volume in curcumin and nanocurcumin group was significantly lower than methotrexate group. However, no significant difference in tumor weight was observed between methotrexate and curcumin group. In nanocurcumin group, it was found to be profoundly lower in tumor weight than other two treatment groups (Fig. 5).

Cytology

Cytology of the ascitic fluid from the treatment group showed features like cell shrinkage, membrane blebbing, cytoplasmic vacuolation, chromatin condensation and nuclear fragmentation. Percentage of apoptotic cells was higher in nanocurcumin group than in curcumin and methotrexate group (Fig. 6 A-D).

Histopathology

Histopathological examination of peritoneum and solid tumor showed that neoplastic cells were invading

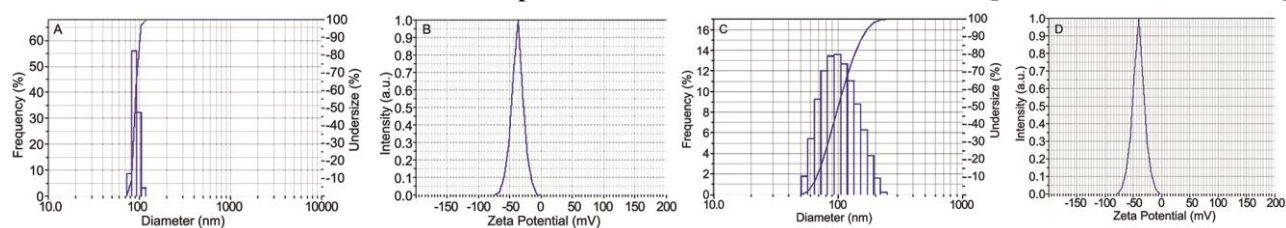


Fig. 1 — (A) Optimized particle size of curcumin solid lipid nanoparticle (CUR-SLN); (B) Zeta potential of CUR-SLN; (C) Optimized particle size of Blank SLN; and (D) Zeta potential of Blank SLN

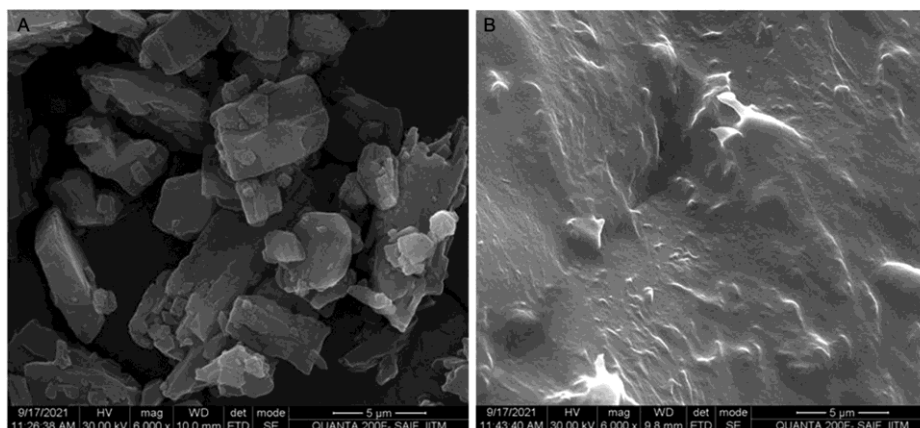


Fig. 2 — Scanning Electron Microscope image of (A) Curcumin showing rough surface; and (B) CUR-SLN showing smooth surface

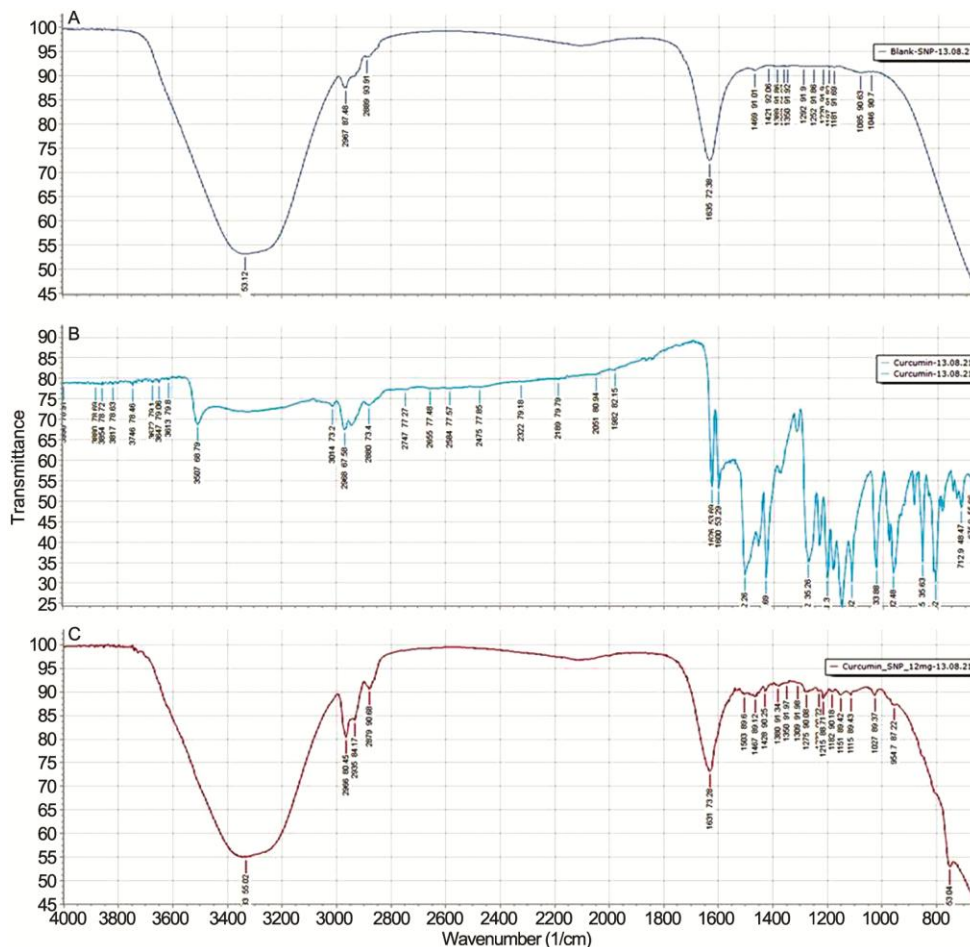


Fig. 3 — Fourier-transform infrared spectroscopy (FTIR) (A) Blank-SLN; (B) Curcumin; and (C) CUR-SLN

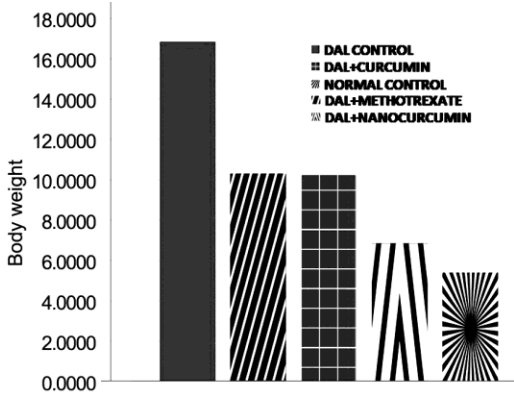


Fig. 4 — Graph representing increase in body weight in different groups

in to the underlying muscle layer in tumor control group with increased vascularity and leukocytic infiltration. In treatment group there was less invasion of neoplastic cells in to the adjacent muscle tissue and decreased number of blood vessels with the tumor tissue. Large areas of necrosis also observed. Numbers of apoptotic cells were more in treatment

group and showed characteristic features like vacuolated cytoplasm, condensation of chromatin and fragmented nuclei (Fig. 6 E-L).

Inhibiting angiogenesis

Visible observation demonstrated the increased vascularity in tumor control group as compared to normal control animals. Treatment groups showed decreased vascularity. Measurement of Microvessel density on H&E sections and anti CD31 immunostained sections increased significantly ($P < 0.05$) in DAL control group (23.33 ± 1.54) when compared to normal control groups (2.17 ± 0.477). Treatment with nanocurcumin showed better reduction in MVD (6.00 ± 0.577) than other groups. Diameter of microvessels also showed significant differences. Tumor control group revealed increased diameter ($18.07 \pm 2.01 \mu\text{m}$) and treatment groups showed significant ($P < 0.05$) reduction in the micro vessel diameter. Nanocurcumin group showed better reduction in diameter ($7.60 \pm 0.57 \mu\text{m}$).

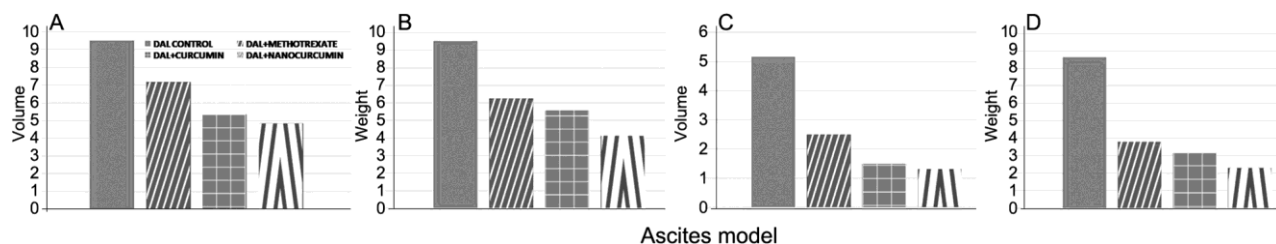


Fig. 5 — Decrease in (A & B) tumor volume and weight in Ascites model; and (C & D) tumor volume and weight in solid tumor model

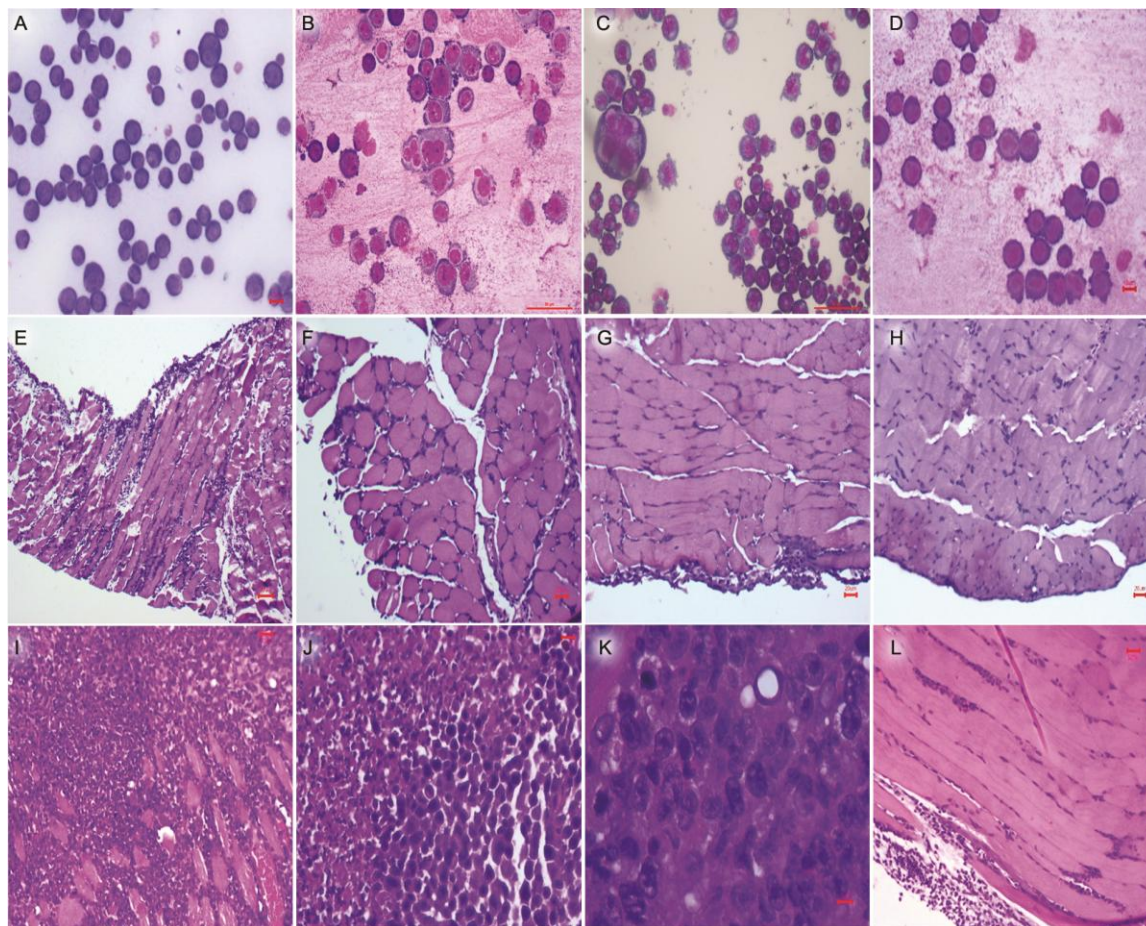


Fig. 6 — (A) Cytology-Tumor control group-Pleomorphic lymphoblast. LG, Bar 10 μ m; (B) Methotrexate Gp- Apoptotic cells. LG, Bar 5 μ m; (C) Curcumin Gp- More apoptotic cells - Membrane blebbing and disruption. LG, Bar 10 μ m; (D) Nanocurcumin Gp- Apoptotic cells-Membrane blebbing. LG, Bar 10 μ m; (E) Ascites model: DAL control Gp- Peritoneal membrane- More invasion of tumor cells. H&E, Bar 20 μ m; (F) Methotrexate Gp- Peritoneal membrane- Minimal invasion of tumor cells. H&E, Bar 20 μ m; (G) Curcumin Gp- Peritoneal membrane-Less invasion of tumor cells. H&E, Bar 20 μ m; (H) Nanocurcumin Gp- Peritoneal membrane- Less invasion of tumor cells. H&E, Bar 20 μ m; (I) Solid model (SM): DAL control- Solid sheets of lymphoblast. H&E, Bar 10 μ m; (J). Methotrexate Gp- Extensive necrosis and apoptosis. H&E, Bar 10 μ m; (K) Curcumin Gp- Apoptotic cells- Nuclear vacuolations. H&E, Bar 5 μ m; and (L) Nanocurcumin Gp- Decreased invasion of tumor cells. H&E, Bar 20 μ m

Immunostaining

Anti-invasive and anti-angiogenic effect were investigated by assessing the expression of CD31, MMP9, COX2 and Nf-kB markers. In tumor control group, the MMP9 and COX 2 showed intense cytoplasmic expression. In treatment groups, there were mild to moderate expression of MMP9 and COX 2.

in DAL control group, there were numerous micro vessels of varying size and shape showed intense CD31 immunoreactivity. In the treatment group, number of blood vessels and intensity of CD31 immunoreactivity were reduced. The immunoreactivity of Nf-kB was more in nucleus in tumor group and cytoplasmic in the treatment group (Fig. 7).

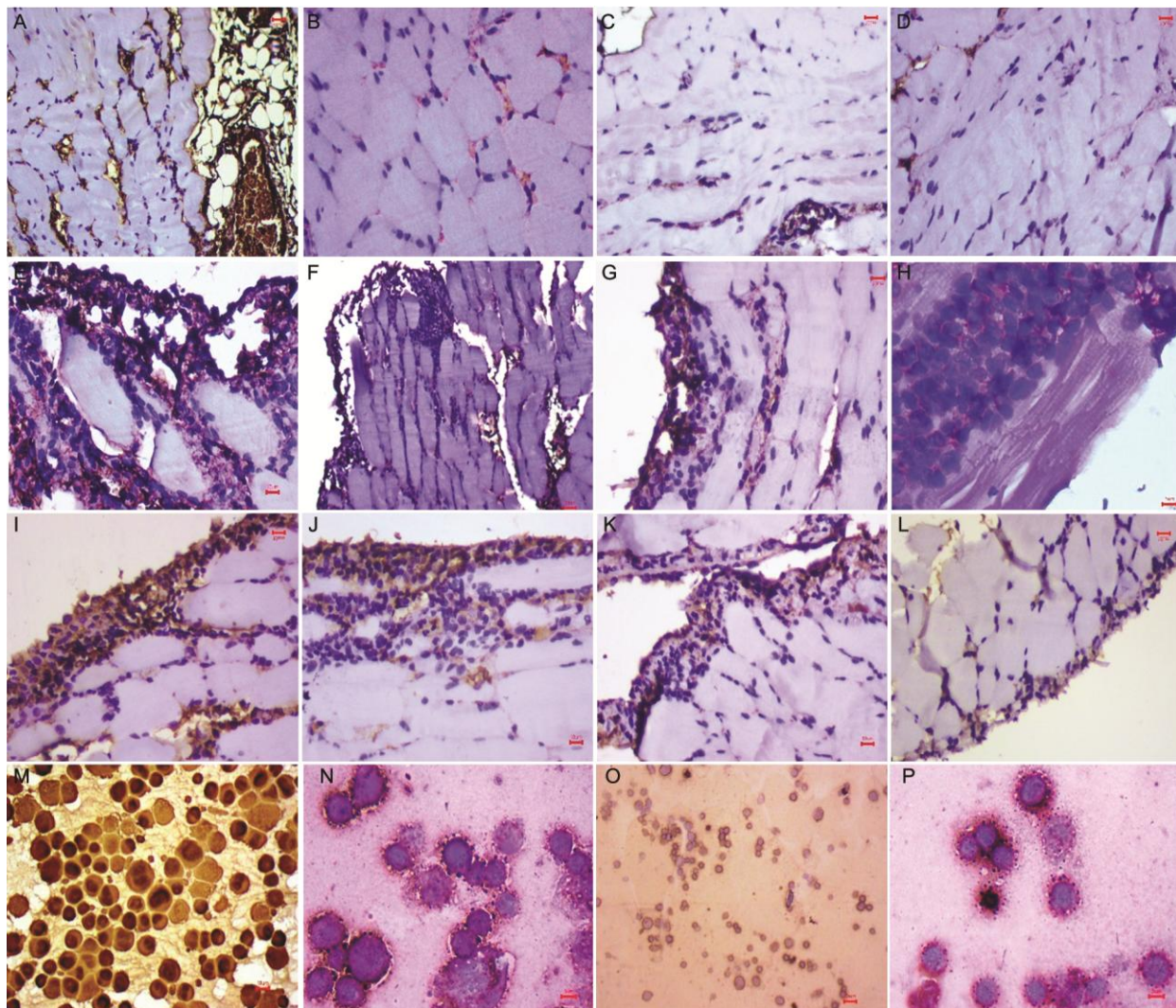


Fig. 7 — (A) Ascites model. Tumor control Gp-Peritoneum-IHC-CD31 Intense cytoplasmic expression in many blood vessels. Bar 20 μm ; (B) Methotrexate Gp-Peritoneum-IHC-CD31 Decreased cytoplasmic expression. Bar 10 μm ; (C) Curcumin Gp- Peritoneum -IHC-CD31 Decreased cytoplasmic expression. Bar 10 μm ; (D) Nanocurcumin Gp- Peritoneum IHC-CD31 Decreased cytoplasmic expression. Bar 10 μm ; (E) DAL Gp- Peritoneum-IHC-MMP9 Intense cytoplasmic expression. Bar 10 μm ; (F) Methotrexate Gp-Peritoneum-IHC-MMP9-Mild cytoplasmic expression. Bar=10 μm ; (G) Curcumin Gp- Peritoneum - IHC-MMP9- Mild cytoplasmic expression. Bar 10 μm ; (H) Nanocurcumin Gp-Peritoneum-IHC-MMP9-Mild cytoplasmic expression. Bar 5 μm ; (I) COX2: DAL Gp- Peritoneum - Increased intense cytoplasmic expression- Bar 10 μm ; (J) Methotrexate Gp- Peritoneum - IHC-COX2 -Mild cytoplasmic expression. Bar 10 μm ; (K) COX2: curcumin Gp- Peritoneum - Mild cytoplasmic expression. Bar 10 μm ; (L) COX2: Nanocurcumin Gp- Peritoneum - Mild cytoplasmic expression. Bar 10 μm ; (M) DAL Gp-ICC- Nf-kB - Intense nuclear expression. Bar 10 μm (N) Methotrexate Gp-ICC- Nf-kB - Intense cytoplasmic expression. Bar 5 μm ; (O) curcumin Gp-ICC-Nf-kB- Intense cytoplasmic expression. Bar 10 μm ; and (P) Nanocurcumin Gp-ICC- Nf-kB- Intense cytoplasmic expression. Bar 5 μm

Mean survival time

Prolongation of lifespan is one of the important criteria to assess the anticancer activity of a drug. The MST in case of tumor control group was found to be 20 and 32 days in ascites model and solid tumor model, respectively. Treatment groups showed significant increase in mean survival time (MST) and percentage increase in lifespan (ILS). Among the three treatment groups nanocurcumin group was

found to be more effective with MST increased to 44 and 49 days in ascites and solid model (Table 1 and Fig. 8).

Discussion

The use of plant-based products to treat cancer had gained importance in recent years owing to their ability to act on multiple signaling pathways. Curcumin is considered as a safe compound and has

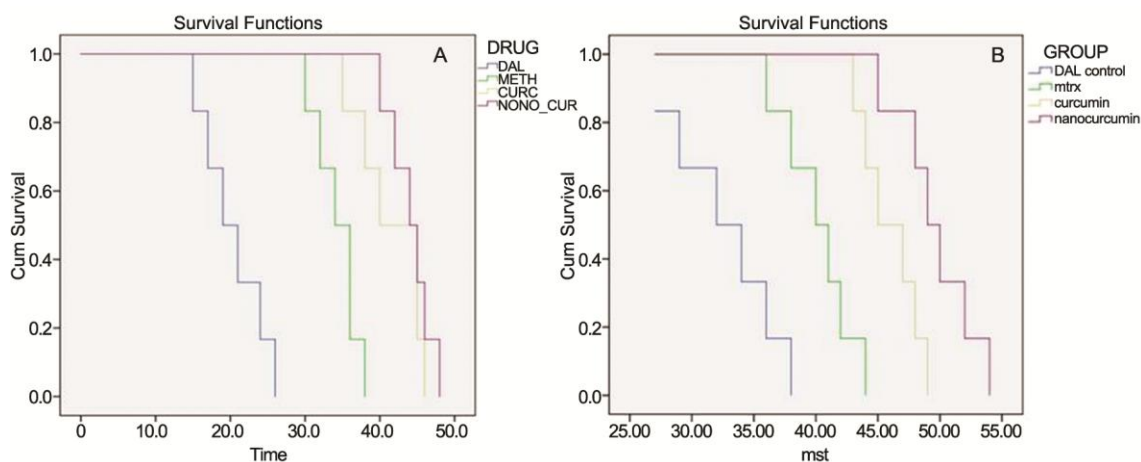


Fig. 8 — Kaplan Meier curve for (A) ascites model; and (B) solid model

been shown to control various signaling molecules at the molecular level. Thus, it can act on multiple cellular pathways¹⁵. Despite having potential health benefits physicochemical instability, low pharmacokinetics and bioavailability, poor bioactive absorption and rapid metabolism limit its clinical use. Integrating curcumin in to nanocarriers was found to be an appropriate choice to increase the bioavailability and solubility, long time circulation and retention in the body¹⁶. The bioavailability of free curcumin increased by 69.78 times when encapsulated in lipid nano constructs as well as there was controlled release of drug in which release extended up to 120 h instead of 24 h in free curcumin¹⁷. In the present study, curcumin was encapsulated in solid lipid nanoparticles by single solvent emulsification evaporation method in which glyceryl monostearate was used as the lipid source. The major advantage of this method of preparation as compared to other methods was that the thermal degradation of the drug can be avoided¹⁸. Previous studies have shown that curcumin have maximum solubility in glyceryl monostearate when panels of lipids are compared^{17,19}.

Particle size is an important parameter that has profound effect on treatment because of larger surface area, high drug loading capacity and controlled drug release. Nanoparticles of size less than 200 nm was found to persist in the circulation for longer time and accumulate in the tumor regions due to enhanced permeation effect²⁰. Consistent to this in the present study, the particle size obtained was 91.1 ± 7.5 nm for CUR-SLN and 106.7 ± 34.9 nm for Blank-SLN. The PDI of the blank solid lipid nanoparticles was 0.319 and for curcumin SLN was 0.367. Poly dispersity index

less than 0.3 indicate the lower aggregation of particles^{21,22}. The storage stability of nanoparticles was found to be related to the zeta potential. Negative zeta potential value observed in this study (-37.6 mv) favour enhanced permeation effect and can evade the identification by the phagocytic system as reported earlier²⁰. FTIR analysis showed that curcumin solid lipid nanoparticles form peak at 3355 cm^{-1} indicating intermolecular stretching of OH group which was absent in curcumin which is a direct indication of formation of solid lipid nanocurcumin¹⁷.

To prove the anticancerous effect in vivo studies were conducted in DAL induced ascites and solid tumor models. Danduga *et al.*²³ suggested that curcumin at 100 mg/kg body wt. provide better anticancerous effect than 50 mg/kg body wt. Kakkar *et al.*²⁴ evaluated the oral bioavailability of CUR-SLN and observed that at 50 mg/kg body wt. the bioavailability increased by 39 times as compared to free curcumin in same dose. Based on these previous reports, here, we compared the antitumor effect of CUR-SLN given at 50 mg/kg body wt. and curcumin at 100 mg/kg body wt. The anticancer effect was assessed by using various parameters like bodyweight, tumor volume and weight, mean survival time and percentage increase in lifespan. In DAL induced animals there was an increase in the bodyweight, tumor volume and weight. It was an indication of cancer progression. Ascitic fluid is the nutritional source for the growth of cancer cells and rapid increase in the ascitic fluid with the tumour growth would be a means to meet the nutritional requirement of tumour cells²⁵. Tumor cells can secrete the vascular permeability factors that promote

accumulation of ascitic fluid and may cause metastasis²⁶. The increase in bodyweight might be due to accumulation of ascitic fluid¹¹. In the treatment groups, there was a significant reduction in the ascitic fluid volume therefore the bodyweight gain was also found decreased which demonstrated the antiproliferative effect of curcumin and nanocurcumin in which later showed better effect. Reduction in tumour volume and tumour weight could be a direct cytotoxic effect on tumour cells or indirect local effect involving macrophage activation and vascular permeability inhibition. To investigate whether the inhibitory effect was local or systemic the effect was tested against solid tumor induced by DAL cell lines. We observed a significant reduction in tumor volume and weight in curcumin and nanocurcumin treated groups when compared to tumor control clearly indicated that the effect is systemic not only related to local effect²⁷. The inhibitory effect of nanocurcumin was found to be comparable with the result produced by standard drug methotrexate.

It is well known that cancer leads to alteration in cellular homeostasis and that disrupts balance between cell proliferation and apoptosis. Evasion of apoptosis is a hall mark of cancer. Ability to induce apoptosis is one of the important criteria for assessing the antitumor effect. Defect in the apoptotic cascade can lead to treatment failure and drug resistance²⁸. Apoptosis or programmed cell death is morphologically characterized by cell shrinkage, cytoplasmic blebbing and chromatin condensation²⁹. Cytology of the ascitic fluid showed similar morphological features indicates the apoptosis inducing property of curcumin.

Angiogenesis is an integral part of tumor development and metastasis which include the development of new blood vessels from the existing vessels. Tumor development induces angiogenic response, an early event in tumor progression. Anti-angiogenic effect of nanocurcumin and curcumin was investigated in murine ascites lymphoma model. Microvessel density could be used as a surrogate measure of assessing angiogenesis in tumor models and could be correlated to the outcome of many tumors³⁰. Intra-tumoral microvessel density was found to be related to regional or distant metastasis of the solid tumors and determination of angiogenesis helps in predicting the response to some forms of conventional anticancer therapy³¹. CD31 expression is

used to assess microvessel density. Nagy et al.³² reported an increase in cross sectional area of the peritoneal blood vessels along with increase in the number of microvessels. In vivo experiments in this study have shown that higher CD31 expression in tumor control group was associated with increased neovascularization, while the treatment groups showed reduced angiogenesis indicated by decrease in microvessel density, microvessel diameter and reduced expression of CD31. This demonstrates that curcumin and nanocurcumin act as inhibitor of angiogenesis to inhibit the tumor growth in vivo. Histopathological changes observed in the present study indicate the increased angiogenesis and vascular permeability contributing to the increased invasiveness of the tumor cells in to the underlying layers. Less invasiveness along with increased necrosis and apoptosis might be attributed to the anti-angiogenic effect of curcumin and nanocurcumin¹⁴.

In continuation, we checked the expression of pro- and angiogenic markers. Curcumin was found to regulate the activation of Nf-kB, transcription factor whose activation is associated with proliferation, invasion, angiogenesis and apoptosis. It plays a key role in the expression of various tumorigenic and pro angiogenic factors like IL-8, VEGF, MMP-9 and COX 2³³. In the present study, we observed the cytoplasmic localization of Nf-kB in the treatment group and nuclear expression in tumor control group indicating that curcumin and nanocurcumin effectively blocked Nf-kB activation and its nuclear translocation³⁴. The present study results showed that curcumin and nanocurcumin effectively diminished the expression of COX2 and MMP9 in DAL. These results were concurrent with the reports of Vigneswaran et al.¹³, Duan et al.³⁵ and Lin et al.³³. Overall, it shows that curcumin and nanocurcumin exert its antitumor effect by inhibiting angiogenesis by targeting Nf-kB and subsequent lowering of pro angiogenic factors like MMP9 and COX2 and thereby reducing the invasion.

The reliable criteria for judging the value of anticancer drug are prolongation of life span³⁶. In the present study, the mean survival time was 20 and 32 days in ascites and solid tumor model, respectively and it was increased in the treatment groups. Nanocurcumin group showed more mean survival time as compared to curcumin and methotrexate group. Similarly, curcumin and nanocurcumin group

showed significant increase in percentage increase in lifespan as compared to control group. Thus, the present study result suggests that curcumin and nanocurcumin effectively inhibit the tumor cell multiplication in DAL induced mice, and thereby prolonged the lifespan of the animals²².

Conclusion

Results of the present study suggest that encapsulation of curcumin in solid lipid nanoparticles administered at 50 mg/kg effectively improved its therapeutic benefit of curcumin in the treatment of cancer by inhibiting angiogenesis by targeting Nf-κB pathway.

Acknowledgement

Authors thank Tamil Nadu Veterinary and Animal Sciences University, Chennai for providing financial support.

Conflict of Interest

Authors declare no competing interests.

References

- Miranda-Filho A, Piñeros M, Znaor A, Marcos-Gragera R, Steliarova-Foucher E & Bray F, Global patterns and trends in the incidence of non-Hodgkin lymphoma. *Cancer Causes Cont*, 30 (2019) 489.
- Siegel RL, Miller KD, Fuchs HE & Jemal A, Cancer statistics, 2022. *CA Cancer J Clin*, 72 (2022) 7.
- Estanqueiro M, Amaral MH, Conceição J & Lobo JM, Nanotechnological carriers for cancer chemotherapy: the state of the art. *Colloids Surf B*, 126 (2015) 631.
- Hesari A, Azizian M, Sheikhi A, Nesaei A, Sanaei S, Mahinparvar N, Derakhshani M, Hedayt P, Ghasemi F & Mirzaei H, Chemopreventive and therapeutic potential of curcumin in esophageal cancer: Current and future status. *Int J Cancer*, 144 (2019) 1215.
- Aggarwal S, Ichikawa H, Takada Y, Sandur SK, Shishodia S & Aggarwal BB, Curcumin (diferuloylmethane) down-regulates expression of cell proliferation and antiapoptotic and metastatic gene products through suppression of IκBα kinase and Akt activation. *Mol Pharmacol*, 69 (2006) 195.
- Das L & Vinayak M, Anti-carcinogenic action of curcumin by activation of antioxidant defence system and inhibition of NF-κB signalling in lymphoma-bearing mice. *Biosci Rep*, 32 (2012) 161.
- Mohanty C & Sahoo SK, The *in vitro* stability and *in vivo* pharmacokinetics of curcumin prepared as an aqueous nanoparticulate formulation. *Biomaterials*, 31 (2010) 6597.
- Shaikh J, Ankola DD, Beniwal V, Singh D & Kumar MR, Nanoparticle encapsulation improves oral bioavailability of curcumin by at least 9-fold when compared to curcumin administered with piperine as absorption enhancer. *Eur J Pharm. Sci*, 37 (2009) 223.
- Bayón-Cordero L, Alkorta I & Arana L, Application of solid lipid nanoparticles to improve the efficiency of anticancer drugs. *Nanomaterials*, 9 (2019) 474.
- Pooja D, Tunki L, Kulhari H, Reddy B.B & Sistla R, Optimization of solid lipid nanoparticles prepared by a single emulsification-solvent evaporation method. *Data Br*, 6 (2016) 15
- Loganayaki N & Manian S, Antitumor activity of the methanolic extract of *Ammannia baccifera* L. against Dalton's ascites lymphoma induced ascitic and solid tumors in mice. *J Ethnopharmacol*, 142 (2012) 305.
- Bancroft JD & Gamble M, *Theory and practice of histological techniques* 6th Edn. (Churchil Living Stone, Newyork), 2008, 53
- Vigneshwaran V, Thirusangu P, Vijay Avin BR, Krishna V, Pramod SN & Prabhakar BT, Immunomodulatory glc/man-directed Dolichos lablab lectin (DLL) evokes anti-tumour response *in vivo* by counteracting angiogenic gene expressions. *Clin Exp Immunol*, 189 (2017) 21.
- Debnath S, Mukherjee A, Karan S, Debnath M & Chatterjee TK, Induction of apoptosis, anti-proliferation, tumor-angiogenic suppression and down-regulation of Dalton's Ascitic Lymphoma (DAL) induced tumorigenesis by poly-l-lysine: A mechanistic study. *Biomed Pharmacother*, 102 (2018) 1064.
- Paulraj F, Abas F, Lajis NH, Othman I & Naidu R, Molecular pathways modulated by curcumin analogue, diarylpentanoids in cancer. *Biomolecules*, 9 (2019) 270.
- Karthikeyan A, Senthil N & Min T, Nanocurcumin: a promising candidate for therapeutic applications. *Front Pharmacol*, 11 (2020) 487.
- Gupta T, Singh J, Kaur S, Sandhu S, Singh G & Kaur IP, Enhancing bioavailability and stability of curcumin using solid lipid nanoparticles (CLEN): A covenant for its effectiveness. *Front Bioeng Biotechnol*, 8 (2020) 879.
- Duong VA, Nguyen TT & Maeng HJ, Preparation of solid lipid nanoparticles and nanostructured lipid carriers for drug delivery and the effects of preparation parameters of solvent injection method. *Molecules*, 25 (2020) 4781.
- Shrotriya S, Ranpise N, Satpute P & Vidhate B. Skin targeting of curcumin solid lipid nanoparticles-engrossed topical gel for the treatment of pigmentation and irritant contact dermatitis. *Artif Cells, Nanomed Biotechnol*, 46 (2018) 1471.
- Kumari M, Sharma N, Manchanda R, Gupta N, Syed A, Bahkali AH & Nimesh S, PGMD/curcumin nanoparticles for the treatment of breast cancer. *Sci Rep*, 11 (2021) 1.
- Tiyaboonchai W, Tungradit W & Plianbangchang P, Formulation and characterization of curcuminoids loaded solid lipid nanoparticles. *Int J Pharm*, 337 (2007) 299.
- Yusuf M, Khan M, Khan RA & Ahmed B, Preparation, characterization, *in vivo* and biochemical evaluation of brain targeted Piperine solid lipid nanoparticles in an experimentally induced Alzheimer's disease model. *J Drug Target*, 21(2013)300.
- Danduga RCSR, Kola PK. & Matli B, Anticancer activity of curcumin alone and in combination with piperine in Dalton lymphoma ascites bearing mice. *Indian J Exp Biol*, 58 (2020) 181.
- Kakkar V, Singh S, Singla D & Kaur IP, Exploring solid lipid nanoparticles to enhance the oral bioavailability of curcumin. *Mol Nut.food Res*, 55(2011)495.

- 25 Aravind SR & Krishnan LK, Curcumin-albumin conjugates as an effective anti-cancer agent with immunomodulatory properties. *Int. immunopharmacol*, 34(2016)78
- 26 Kasai S, Kuwayama N, Motoo Y, Kawashima A, Matsumoto K, Yano S, Matsushima K & Yasumoto K, Dual blockade of MET and VEGFR2 signaling pathways as a potential therapeutic maneuver for peritoneal carcinomatosis in scirrhous gastric cancer. *Biochem Biophys Res Commun*, 600(2022) 80.
- 27 Sakthivel KM & Guruvayoorappan C. Acacia ferruginea inhibits tumor progression by regulating inflammatory mediators-(TNF- α , iNOS, COX-2, IL-1 β , IL-6, IFN- γ , IL-2, GM-CSF) and pro-angiogenic growth factor-VEGF. *Asian Pac J Cancer Prev*, 14(2013)3909.
- 28 Saini RK, Keum YS, Daglia M & Rengasamy KR. Dietary carotenoids in cancer chemoprevention and chemotherapy: A review of emerging evidence. *Pharmacol Res*, 157 (2020) 104830.
- 29 Shtilbans V, Wu M & Burstein DE, Evaluation of apoptosis in cytologic specimens. *Diagn Cytopathol*, 38 (2010) 685.
- 30 Goddard JC, Sutton CD, Furness PN, Kockelbergh RC & O'byrne KJ, A computer image analysis system for microvessel density measurement in solid tumours. *Angiogenesis*, 5 (2002) 15.
- 31 Hasan J, Byers R & Jayson GC, Intra-tumoural microvessel density in human solid tumours. *Br J cancer*, 86 (2002) 1566.
- 32 Nagy JA, Morgan ES, Herzberg KT, Manseau EJ, Dvorak AM & Dvorak HF, Pathogenesis of ascites tumor growth: angiogenesis, vascular remodeling, and stroma formation in the peritoneal lining. *Cancer Res*, 55 (1995) 376.
- 33 Lin YG, Kunnumakkara AB, Nair A, Merritt WM, Han LY, Armaiz-Pena GN, Kamat AA, Spannuth WA, Gershenson DM, Lutgendorf SK & Aggarwal BB, Curcumin inhibits tumor growth and angiogenesis in ovarian carcinoma by targeting the nuclear factor- κ B pathway. *Clin Cancer Res*, 13 (2007) 3423.
- 34 Belakavadi M & Salimath BP, Mechanism of inhibition of ascites tumor growth in mice by curcumin is mediated by NF- κ B and caspase activated DNase. *Mol Cell Biochem*, 273 (2005) 57.
- 35 Duan J, Zhang Y, Han S, Chen Y, Li B, Liao M, Chen W, Deng X, Zhao J & Huang B, Synthesis and *in vitro/in vivo* anti-cancer evaluation of curcumin-loaded chitosan/poly (butyl cyanoacrylate) nanoparticles. *Int J Pharm*, 400 (2010) 211.
- 36 Sudarsanan D, Suresh Sulekha D & Chandrasekharan G, Amomum subulatum induces apoptosis in tumor cells and reduces tumor burden in experimental animals via modulating pro-inflammatory cytokines. *Cancer Invest*, 39 (2021) 333.